PHYSICAL REVIEW B VOLUME 9, NUMBER 4 15 FEBRUARY 1974

Conduction in quantized silicon inversion layers with many occupied electric subbands

A. R. Nelson* and E. Brown

Physics Department, Rensselaer Polytechnic Institute, Troy, New York 12181

(Received 23 August 1973)

A simple model of the inversion layer is used to compute the electron mobility in quantized silicon surface channels for the case of many occupied electric subbands. Interband scattering is included. Important approximations in the calculation are a triangular surface potential well and a δ-function form for the scattering potential. The results are presented over a broad range of gate voltage and temperature, and the effects of interband scattering are examined. In general, the theoretical predictions are in fairly good agreement with the experimental behavior.

I. INTRODUCTION

An inversion layer is formed when a strong electric field of the proper polarity is applied to the surface of a semiconductor, so that the minority carriers in the bulk become the majority carriers near the surface. In the case of p-type bulk, electrons are held near the interface in a potential well but are free to move parallel to the surface. If the electric field is strong enough, the electron's motion perpendicular to the surface is quantized in discrete energy levels.[1] This has been confirmed by experiments at low temperatures.[2,3] If we include the possibility of motion parallel to the surface (x, y direction), the carrier can be characterized as belonging to particular electric subbands, i.e.,

$$E_{\text{total}}(n, k_x, k_y) = E_n' + E(k_x, k_y),$$

where E_n' is the energy associated with the quantization in the z direction and $E(k_x, k_y)$ corresponds to the free motion along the surface. Most previous discussions[4-7] of possible surface-related scattering mechanisms have been confined to the electric quantum limit. This corresponds to the range of temperatures and electron concentration where only the lowest electric subband is appreciably occupied. Recent experimental studies[8-10] have shown that quantum effects are important at room temperature, in some instances. In these cases, many energy bands are occupied, and the theory of electron conduction becomes much more complicated. (We are not concerned in this paper with the classical approximation, which is valid for weak inversion layers.[11])

In the past several years, theoretical formalisms have been developed to deal with conduction in quantized inversion layers of semiconductors with many occupied electric subbands.[12,13] However, actual comparison with experiments[14] has not been carried out. Our purpose in this paper is to make an initial attempt at bridging the gap between abstract formalism and comparison with experimental results. In particular, we are interested in examining effects related to many-band conduction and interband scattering. To this end, we apply the many-band theory of Siggia and Kwok,[12] which includes interband scattering, using a simple model of the inversion layer. We calculate electron mobility and are able to make a reasonable comparison with experiment over a fairly wide range of temperature and carrier concentration.

II. PROCEDURE

We assume that the electrons are trapped near the surface in a triangular well, i.e.,

$$\begin{aligned} V(z) &= eFz, \quad z > 0, \\ V(z) &= \infty, \quad z < 0, \end{aligned} \tag{1}$$

where V is the potential energy of the electron, z is the coordinate perpendicular to the surface, and F is some average electric field seen by the mobile electrons in the inversion layer. An accurate treatment of the inversion-layer potential, energy levels, and wave functions involves, among other things, the self-consistent solution of the Schrödinger equation with Poisson's equation. Our assumption of the triangular well reduces the amount of calculation considerably but may affect our results for strong inversion layers. Stern[15] has examined the validity of the linear-potential method as compared with more accurate treatments.

Proceeding, we may write the effective field F in the form

$$F = (4\pi e/\kappa_s)(gN_{\text{inv}} + N_A d), \tag{2}$$

where N_{inv} is the number of electrons in the inversion layer per unit area, N_A is the volume density of acceptors, d is the width of the depletion layer, and g is a factor arising from the self-screening effect of the electrons. Consistent with our linear-potential approximation, the exact value of g is not important in our calculation, and we set $g = \frac{11}{32}$, as first done by Uemura and Matsumoto.[6]

We use the effective-mass approximation. For each valley or energy ellipsoid which originates in the bulk, we have

$$H = P_x^2/2m_x + P_y^2/2m_y + P_z^2/2m_z + V(z) , \quad (3)$$

where m_x, m_y, and m_z are the effective masses for the three coordinate directions and depend upon the particular valley we wish to describe with our effective-mass Hamiltonian H. The eigenfunctions of H are the product of a free-electron portion $e^{ik_x x + ik_y y}$ for the motion parallel to the surface and a z-dependent factor $\psi_n(z)$, which satisfies

$$H'\psi_n(z) = E_n'\psi_n(z) , \quad (4)$$

where

$$H' = P_z^2/2m_z + V(z) . \quad (5)$$

The total energy of an electron in the nth band is

$$E_{\text{total}}(n, k_x, k_y) = E_n' + \hbar^2 k_x^2/2m_x + \hbar^2 k_y^2/2m_y . \quad (6)$$

If the potential $V(z)$ is linear, then Eq. (4) may be cast in the form of the Airy equation, whose solution is well known.[15,16] The normalized eigenfunctions $\psi_n(z)$ are

$$\psi_n(z) = \left(\frac{(a)^{1/2}}{\text{Ai}'(b_n)}\right)\text{Ai}(az + b_n), \; z > 0; \; \psi_n(z) = 0, \; z < 0; \quad (7)$$

where

$$a = (2m_z eF/\hbar^2)^{1/3}, \quad (8)$$

$$b_n = -aE_n'/eF, \quad (9)$$

Ai is the Airy function, and $\text{Ai}'(b_n)$ is the derivative of Ai evaluated at $z = 0$. A simple asymptotic expression for large n exists for E_n',

$$E_n' \simeq (\hbar^2/2m_z)^{1/3}\left[\tfrac{3}{2}\pi eF(n + \tfrac{3}{4})\right]^{2/3} . \quad (10)$$

In calculating the transport properties, we must also consider the multiple-valley structure of silicon. In the bulk, the conduction band has six equivalent minima along the $\pm k_x$, $\pm k_x$, and $\pm k_z$ axes. This will lead to different physical properties, depending on the surface we are considering. For a (100) surface, for example, there are actually two ladders of energy bands. These correspond to the two different values of m_z possible in the effective-mass approximation with the six different ellipsoids. The lowest set of energy levels has $m_z = 0.98\,m_e$ and is twofold degenerate, while the set of levels which are higher in energy have $m_z = 0.19\,m_e$ and are fourfold degenerate (not including spin degeneracy). The energy levels and wave functions for these two sets of bands are given by Eqs. (7)–(10), using the appropriate value of m_z.

We consider a system of independent scatterers. The potential V due to the scatterer at the site $\vec{R}_j$ is of the δ function or "contact-potential" form, i.e.,

$$V = V_0\,\delta(\vec{r} - \vec{R}_j),$$

where V_0 is an adjustable strength parameter. (We will discuss this choice of potential further in Sec. IV.) It is assumed that there is a uniform volume density of these scatterers in the bulk, and this density has been set equal to N_A. In addition, we use a separate interface density N_{int} in order to model scattering by the surface or mechanisms associated with the surface. This ratio of interface to bulk scattering can, of course, be varied to test the relative importance of surface-related scattering.

The model of the inversion layer described above is used to calculate the mobility. We use the formulas developed by Siggia and Kwok.[12] They make use of a Boltzmann-equation analysis to set up a system of coupled differential equations and reduce the problem by introducing a relaxation time for each band. Our procedure consists of evaluating their expressions for the conductivity, essentially Eqs. (88), (89), and (91) in their paper, using the wave functions, energy levels, scattering potential, and distribution of scatterers previously described in this article. We do not consider intervalley scattering. Instead, we evaluate the mobility corresponding to each constant energy ellipsoid separately and then average appropriately. For δ-function scatterers, intervalley scattering contributes in the same way as interband scattering and involves a great deal of additional calculation, while revealing no new effects.

It is also necessary in the calculation to obtain the position of the Fermi level, E_F, relative to the various ladders of energy bands. This can be found by solving numerically

$$N_{\text{inv}} = 2\sum_{\nu, n, \vec{k}} f_n^\nu(\vec{k}) = kT\sum_\nu\left(D^\nu\sum_n \ln(1 + \exp\gamma_n^\nu)\right) ,$$

where

$$\gamma_n^\nu = (E_F - E_{\text{min}}^{n,\nu})/kT,$$

and $E_{\text{mim}}^{n,\nu}$ is the minimum energy of the nth band and νth valley. The distribution function $f_n^\nu(\vec{k})$ is the Fermi-Dirac function in two-dimensional k space, k_x and k_y. The density of states D^ν for each two-dimensional subband is a constant, given by

$$D^\nu = 2(m_x^\nu m_y^\nu)^{1/2}/\pi\hbar^2,$$

where the effective masses depend on the valley under consideration.

The number of bands needed in the calculation depends on the electric field F and the temperature under consideration. At room temperature, we used up to 25 bands for each valley. According to the triangular-well model, this takes into account about 90% of the electrons in the inversion layer for the weaker values of the electric field.

III. RESULTS

In order to obtain numerical values for the mobility, it is necessary to assume a value for V_0, the strength of the δ-function potential. In the calculation, this parameter V_0 becomes a constant factor multiplying the mobility. The magnitude of V_0 (5.5×10^{-20} eV cm^3) was chosen so as to give the best agreement with experimental results. However, it should be pointed out that this same value was always used and was not changed for each comparison.

Figure 1 shows the theoretical behavior found when the surface electric field or inversion-layer electron concentration is varied at room temperature. Between $N_{inv}=10^{10}$ cm^{-2} and $N_{inv}=10^{11}$ cm^{-2}, the mobility is nearly constant because the surface electric field is relatively unchanged in this region. This is due to the fact that the depletion-layer charge is approximately 10^{11} cm^{-2}, for this sample, and dominates the magnitude of the surface electric field for small N_{inv}.

Above $N_{inv}=10^{11}$ cm^{-2}, the increasing field is responsible for two main effects. When the electric field is made stronger, the separation between the energy-band minima increases due to the larger steepness of the potential well. This increased separation of the levels means less interband scattering, and, therefore, an increase in the mobility with field. This explains the curve in Fig. 1 that does not include surface scattering (labeled $N_{int}=0$). However, the inclusion of surface scattering introduces another effect which may be stronger, depending on the value of N_{int}. A stronger field pulls the electrons closer to the interface and lowers the mobility. This is shown by the lower decreasing curve in Fig. 1, which corresponds to $N_{int}=10^{12}$ cm^{-2}. Also shown in the figure is a curve for the case of no interband scattering. The mobility is much higher for a given N_{inv}, but decreases very rapidly as the field increases.

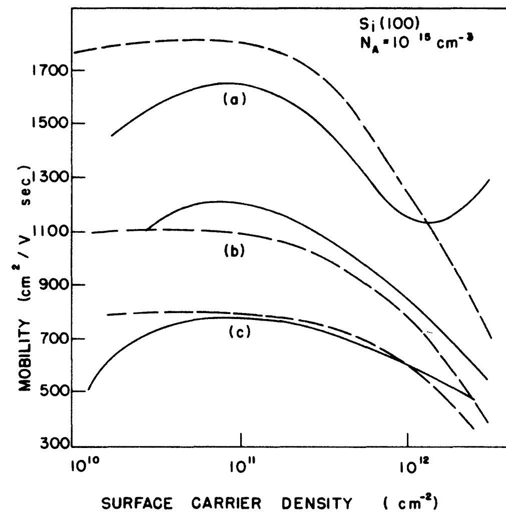

FIG. 2. Experimental (solid line) and theoretical (dashed line) values of mobility versus carrier concentration for three values of temperature: (a) $T=90$ °K; (b) $T=192$ °K; (c) $T=295$ °K. Experimental curves from Fang and Fowler (sample 2847F). Theoretical curves computed for $N_{inv}=2\times10^{11}$ cm^{-2}.

In Fig. 2, we compare our calculated field dependence with the Hall mobility found by Fang and Fowler[14] for three different temperatures. The theoretical curves (based on $N_{int}=2\times10^{11}$ cm^{-2})

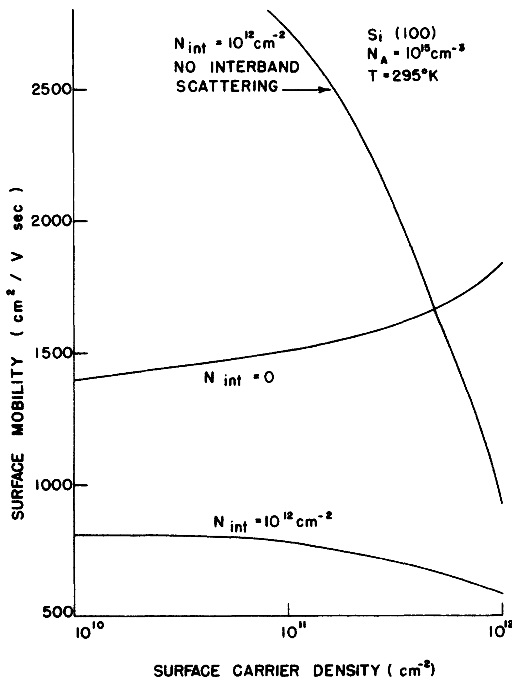

FIG. 1. Theoretical values of mobility vs N_{inv}.

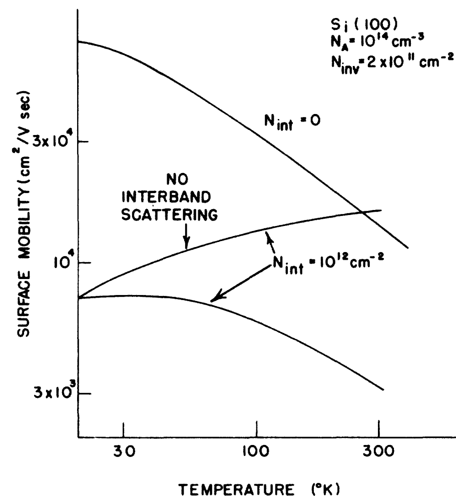

FIG. 3. Theoretical values of mobility vs T.

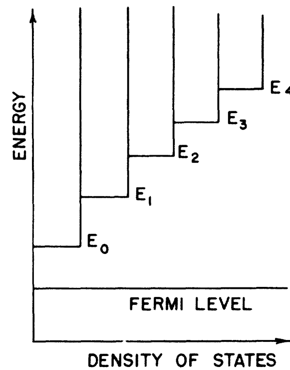

FIG. 4. Density of states versus energy for one ladder of two-dimensional energy bands.

agree well with the field dependence of the experimental results above $N_{inv} = 10^{11}$ cm^{-2}. Below this value, experiments show a mobility that increases with N_{inv}. This has been tentatively explained by Stern and Howard[4] as due to the increase in the shielding of charged scatterers as the electron concentration increases. Of course, this effect is not incorporated in our model. Our model also does not suggest why the mobility rises again above $N_{inv} = 10^{12}$ cm^{-2} at $T = 90$ °K.

The temperature dependence of our calculated mobilities is illustrated in Fig. 3. At very low temperatures, the mobility is almost constant, since most of the electrons are confined to the single lowest band. This constant mobility is a characteristic of the δ-function scattering in two dimensions. As the temperature increases, higher bands are populated, including the lowest energy band corresponding to the valleys with $m_z = 0.19\, m_e$. As previously mentioned, these valleys give rise to a ladder of levels which are higher in energy than the set with $m_z = 0.98\, m_e$. The electrons in these two sets of energy levels have different mobilities for two reasons. There is an increased density of states for the electrons with $m_z = 19\, m_e$ because of the larger mass for motion parallel to the surface. This tends to lower the mobility. However, the average distance from the surface is much larger for the electrons with the lighter effective mass perpendicular to the surface. If the surface scattering is large, this effect will be dominant. This explains why the two curves in Fig. 3 with $N_{int} = 10^{12}$ cm^{-2} show an initial increase in mobility with T, while $N_{int} = 0$ decreases.

As the temperature continues to increase, the effect of interband scattering becomes dominant. This is shown by the two curves with $N_{int} = 10^{12}$ cm^{-2}. The one that does not include interband scattering continuously increases, while the curve with interband interactions begins to decrease. This is because increasing the temperature with fixed gate voltage spreads the electron distribution out into higher bands. (The total number of electrons is fixed by the gate voltage.) Since the density of states available for scattering increases in steps with energy (Fig. 4), the mobility will drop, but only if interband scattering is included. This is consistent with the photoconductive experiments[17] which show a drop in mobility when electrons are excited to upper bands.

In Fig. 5, we compare our values for the temperature dependence with the experimental values of Fang and Fowler.[14] A word of explanation is necessary concerning the experimental mobility curves. Originally, their data for this sample were presented as curves of effective mobility. When plotted versus $e^{-E_a/kT}$, this data gave a straight line at low T. It has been suggested[4,14] that this exponential temperature dependence results from trapping of electrons in bound states. As T increases, these electrons are released with an activation energy equal to E_a, and this changes the number of electrons which are free to conduct a current. Since we are concerned here with the true mobility, it was necessary to multiply the effective mobility by $e^{E_a/kT}$, which has been done in Fig. 5.

The theoretical curves in Fig. 5 show fairly good agreement with the temperature dependence of experiment. They are drawn for the case of $N_{int} = 10^{12}$ cm^{-2}, although approximately the same results can be obtained for $N_{int} = 5 \times 10^{11}$ cm^{-2} to $N_{int} = 2 \times 10^{12}$ cm^{-2}.

IV. DISCUSSION

The results for the many-band calculation presented here follow the general trends of experi-

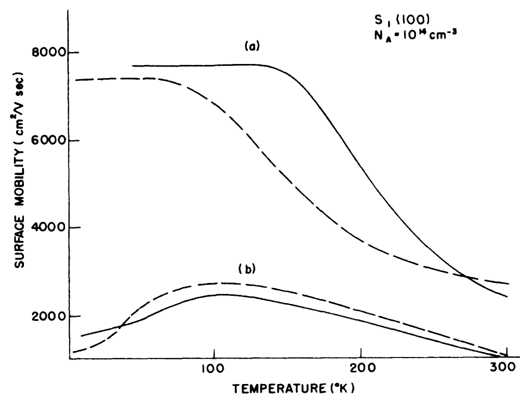

FIG. 5. Experimental (solid line) and theoretical (dashed line) values of mobility versus temperature for two values of N_{inv}: (a) $N_{inv} = 2 \times 10^{11}$ cm^{-2}; (b) $N_{inv} = 6 \times 10^{11}$ cm^{-2}. Experimental curves have been adjusted to give true mobility from Fang and Fowler's measured effective mobility (sample 3777). Theoretical curves computed for $N_{inv} = 10^{12}$ cm^{-2}.

ment over a fairly wide range of electric field, temperature, and bulk doping. However, the use of a δ-function scattering potential makes the interpretation of this agreement somewhat difficult. The δ function may be a good model for a short-ranged scattering process, such as a neutral impurity or surface roughness. This may not be the case for screened impurity charges, however. Calculations by Stern and Howard[4] show that oxide charges may have a fairly long range in the surface layer for some electron concentrations. This may be of particular importance when we consider interband scattering, since the wave functions for different bands are orthogonal. A long-ranged smoothly varying potential will then lead to a greatly reduced matrix element between wave functions.[13] For a short-ranged scatterer, the orthogonality is not of such great importance.

Of course, at the present time, there is reasonable evidence for the importance of several different scattering processes from the single-band calculations which have been carried out to date.[18,19] As previously mentioned, the screened-impurity model[4] seems to explain the increase in mobility with field which occurs at smaller electron concentrations. In addition, other investigators[20–22] have had some success by considering the effect on mobility of the potential fluctuation due to a random distribution of ionized impurities near the interface. For larger inversion-layer concentrations, there is good experimental evidence[7] that the sharp decrease in mobility with field is due to surface roughness. Also, a single-band calculation for surface phonons[5] yields approximately the correct decrease with F and T found experimentally at high fields and room temperature. The magnitude obtained for the mobility is about an order of magnitude too high, but the inclusion of higher occupied subbands, with interband and intervalley scattering, might very well correct this discrepancy. Both acoustical and optical phonons are considered in another treatment.[21]

Thus, there is a good deal of evidence that a proper comprehensive treatment of scattering in the inversion layer will be extremely complicated. Accordingly, it is not possible to associate the δ function used here with any particular mechanism. However, we can note that it was not possible to obtain agreement with experiment without both a bulk distribution and a surface density of scatterers. In fact, the best value of N_{int} for our calculations is of the same order of magnitude as the surface density of oxide charges for these samples, but it is not known if this is significant.

We are also able to conclude that interband scattering is an important process limiting the mobility in inversion layers. In particular, it causes a sharp reduction in mobility for higher temperatures, at least for a short-ranged scattering process. Calculations of multiband conduction with a more realistic treatment of the electron scattering process are planned for the future.

ACKNOWLEDGMENTS

The authors wish to thank Dr. F. Stern and Dr. A. B. Fowler for the useful articles and information supplied by them.

---

*Present address: Solid State Sciences Laboratory, Air Force Cambridge Research Laboratories, Bedford, Mass. 01730.

[1]For a review article on quantum effects in inversion layers, see F. Stern, in *Proceedings of the Tenth International Conference on the Physics of Semiconductors, Cambridge, Massachusetts*, 1970 (U. S. Atomic Energy Commission, Oak Ridge, Tenn., 1970), p. 451.

[2]F. F. Fang and W. E. Howard, Phys. Rev. Lett. 16, 797 (1966).

[3]A. B. Fowler, F. F. Fang, W. E. Howard, and P. J. Stiles, Phys. Rev. Lett. 16, 901 (1966).

[4]F. Stern and W. E. Howard, Phys. Rev. 163, 816 (1967).

[5]S. Kawaji, H. Ezawa, and K. Nakamura, J. Vac. Sci. Technol. 9, 762 (1972); H. Ezawa, S. Kawaji, and K. Nakamura (to be published).

[6]Y. Uemura and Y. Matsumoto, Jap. J. Appl. Phys. Suppl. 40, 205 (1971).

[7]Y. C. Cheng and E. A. Sullivan, Surface Sci. 34, 717 (1973).

[8]J. A. Pals, Phys. Rev. B 5, 420 (1972).

[9]H. Sakaki and T. Sugano, in *Proceedings of the Third Conference on Solid State Devices, Tokyo*, 1971 (unpublished), p. 141.

[10]H. Sakaki and T. Sugano, Jap. J. Appl. Phys. 10, 1016 (1971).

[11]See, e.g., D. R. Frankl, *Electrical Properties of Semiconductor Surfaces* (Pergamon, New York, 1967).

[12]E. D. Siggia and P. C. Kwok, Phys. Rev. B 2, 1024 (1970).

[13]M. E. Alferieff and C. B. Duke, Phys. Rev. 168, 832 (1968).

[14]F. F. Fang and A. B. Fowler, Phys. Rev. 169, 619, (1968).

[15]F. Stern, Phys. Rev. B 5, 4891 (1972).

[16]*Handbook of Mathematical Functions*, edited by M. Abramowitz and I. A. Stegun (U. S. GPO, Washington, D. C., 1964).

[17]R. G. Wheeler and R. W. Ralston, Phys. Rev. Lett. 27, 925 (1971).

[18]Y. C. Cheng and E. A. Sullivan, J. Appl. Phys. 44, 923 (1973).

[19]J. L. Rutledge and W. E. Armstrong, Solid-State Electron. 15, 215 (1972).

[20]Y. C. Cheng, J. Appl. Phys. 44, 2425 (1973).

[21]C. T. Sah, T. H. Ning, and L. L. Tschopp, Surface Sci. 32, 561 (1972).

[22]T. H. Ning and C. T. Sah, Phys. Rev. B 6, 4605 (1972).